

UAS-BASED MULTI-ANGULAR REMOTE SENSING OF THE EFFECTS OF SOIL MANAGEMENT STRATEGIES ON GRAPEVINE

Rebecca RETZLAFF^{1*}, Daniel MOLITOR², Marc BEHR², Christian BOSSUNG¹, Gilles ROCK¹, Lucien HOFFMANN², Danièle EVERS² and Thomas UDELHOVEN^{1,2}

1: Universität Trier, FB VI – Geography/Geosciences, Environmental Remote Sensing and Geoinformatics, Campus II, Behringstrasse 21, D-54286 Trier, Germany

2: Environmental Research and Innovation Department, LIST, Luxembourg Institute of Science and Technology, 41, rue du Brill, L-4422 Belvaux, Luxembourg

Abstract

Aims: The present investigation in a Luxembourgish vineyard aimed at evaluating the potential of multispectral, multi-angular UAS (unmanned aerial system) imagery to separate four soil management strategies, to predict physiological variables (chlorophyll, nitrogen, yield etc.) and to follow seasonal changes in grapevine physiology in relation to soil management.

Methods and results: Multi-angular (nadir and 45° off-nadir) multispectral imageries (530-900 nm) were taken in the years 2011 and 2012. Image grey values and reflectance-derived vegetation indices were computed and canopy and vigour properties were monitored in the field. All four soil management strategies could be significantly discriminated (box-plots, linear discriminant analysis) and vegetation properties estimated (linear regression) in 2011. For 2012, global models predicted chlorophyll contents and nitrogen balance index values with a R^2_{cv} of 0.65 and 0.76, respectively.

Conclusions: Soil management strategies strongly affect plant vigour and reflectance. Differences were best detectable by oblique visible/near-infrared (Vis/nIR) UAS data of illuminated canopies.

Significance and impact of the study: UAS imaging is a flexible tool for applications in precision viticulture.

Key words: grapevine physiology, multispectral remote sensing, soil management viewing geometry, unmanned aerial system, vigour, viticulture

Résumé

Objectifs : Cette étude a pour objet d'évaluer le potentiel de l'imagerie multispectrale et multiangulaire d'un drone dans un vignoble luxembourgeois afin de discriminer quatre modes de travail du sol, d'estimer des variables physiologiques (teneur en chlorophylle et en azote, rendement, etc.) et de suivre la physiologie de la vigne en relation avec le mode de travail du sol.

Méthodes et résultats : Les images multiangulaires (nadir et 45°) et multispectrales (530-900 nm) ont été réalisées en 2011 et 2012. Les niveaux de gris des images et plusieurs indices de végétation dérivés de la réflectance ont été calculés ; la vigueur et la structure de la canopée ont été mesurées au vignoble. Les modes de travail du sol peuvent être significativement discriminés par analyse discriminante et les propriétés de la canopée ont été estimées par régression linéaire pour 2011. En 2012, les modèles de prédiction de la teneur en chlorophylle et de l'indice d'équilibre azoté sont caractérisés par des R^2_{cv} de 0.65 et 0.76, respectivement.

Conclusion : Le mode de travail du sol affecte significativement la réflectance du couvert et la vigueur. Ces différences sont bien mises en évidence par les données visibles/proche infra-rouge de l'image oblique de la partie éclairée de la canopée.

Signification et impact de l'étude : L'imagerie par drone est un outil intéressant pour des applications en viticulture de précision.

Mots clés : physiologie de la vigne, imagerie multispectrale à distance, mode de travail du sol, drones, vigueur, viticulture

manuscript received 23rd May 2014 - revised manuscript received 5th January 2015

Introduction

Vineyard soils are the substrate for cultivated grapevines; they allocate moisture and nutrient uptake, influence the microclimate in the canopy and have an impact on the typicity of the wine (Bramley *et al.* 2011a, Jackson and Lombard 1993, Schultz and Löhnertz 2002, Meggio *et al.* 2010, Bramley *et al.* 2011a, Bramley *et al.* 2011b, Tardaguila *et al.* 2011, Arnó *et al.* 2012, Hall and Wilson 2013). Thus, soil management has a direct influence on grape vegetative growth, fruit composition, and finally wine quality. Vineyard soil management comprehends the sowing of cover crops, tilling, mowing and chemical treatments aiming at the suppression of weeds, fostering of nutrient uptake, minimization of water loss and soil erosion, and avoidance of pests and diseases (Tesci *et al.* 2007). Cover crops play an important role for the carbon and water balance of vineyards (Schultz and Stoll 2010). In the late 1980s, however, viticulturists recognized that cover crops also increase competition for nitrogen (N) and water uptake and might contribute to the development of atypical aging flavour, an off-flavour in white wines (Schultz and Löhnertz 2002, Schneider 2010).

Remote sensing constitutes a valuable tool to monitor vineyard properties and to retrieve physiological plant parameters. Chlorophyll (Chl) content (frequently directly linked to grape vigour, growth and yield) turned out to be easily detectable by means of remote sensing (Gil-Perez *et al.* 2010). Due to vineyard architecture, remote sensing of leaf and canopy variables requires large-scale imagery. Traditionally, high spatial resolution satellite imagery such as Ikonos (Johnson *et al.* 2003) and, more so, aerial imagery are used in this context utilising multispectral (Smit *et al.* 2010), hyperspectral (Zarco-Tejada *et al.* 2005, Meggio *et al.* 2008, Gil-Perez *et al.* 2010, Smit *et al.* 2010) and thermal sensors (Berni *et al.* 2009b). Aerial imagery might supply appropriate data, but flight campaigns are expensive and need substantial pre-planning.

In recent years, unmanned aerial systems (UAS) and services are emerging, offering a more operational, low-cost platform which allows retrieving spatial data at times when it is most needed. UAS have recently been applied for deriving biophysical parameters (Suárez *et al.* 2009, Zarco-Tejada *et al.* 2009, Suárez *et al.* 2010, Baluja *et al.* 2012, Primicerio *et al.* 2012, Suárez *et al.* 2009, Suárez *et al.* 2010, Zarco-Tejada *et al.* 2009, Zarco-Tejada *et al.* 2012, Mathews and

Jensen 2013) and for water stress detection in vineyards and tree plantations (Berni *et al.* 2009a, Berni *et al.* 2009b, Berni *et al.* 2009c, Zarco-Tejada *et al.* 2013a).

Also, vegetation indices have been employed to map Chl content and vigour properties: The normalized difference vegetation index, NDVI (Tucker 1979, Huete and Jackson 1988, Tucker 1979), has been applied to mapping wine quality, grapevine vigour (Meggio *et al.* 2010, Primicerio *et al.* 2012), long-term water deficits and stem water potential (Baluja *et al.* 2012). The ratio of the transformed chlorophyll absorption ratio index, TCARI (Haboudane *et al.* 2002), and optimized soil-adjusted vegetation index, OSAVI (Rondeaux *et al.* 1996), TCARI/OSAVI, appropriately estimates stomatal conductance (Baluja *et al.* 2012). The abundance of (narrow-band/hyperspectral) spectral vegetation indices for mapping Chl and plant pigments has been described in detail (Haboudane *et al.* 2002, Zarco-Tejada *et al.* 2004, Zarco-Tejada *et al.* 2005, Gil-Perez *et al.* 2010).

Water stress as well as photosynthetic efficiency may be measured by the narrow-band photochemical reflectance index PRI (Gamon *et al.* 1997, Thenot *et al.* 2002, Berni *et al.* 2009b, Suárez *et al.* 2009, Suárez *et al.* 2010). However, the PRI has also been proven to be sensitive to differences in crown-structure, viewing and illumination geometry, showing the strongest response in illuminated hot spot conditions and shadowed canopy (Hall *et al.* 2008, Hilker *et al.* 2008, Zarco-Tejada *et al.* 2013b).

Therefore, recent studies combined the renormalized difference vegetation index, RDVI (Roujean and Breon 1995), and the red edge ratio (ρ_{700}/ρ_{670}) as a normalization factor to the PRI, obtaining an indicator sensitive not only to water stress but also to canopy Chl content (Zarco-Tejada *et al.* 2013a).

Different soil management strategies have not yet been studied by multispectral remote sensing in more detail under cool climate viticulture conditions. Our objectives were: (i) to assess if soil management strategies can be separated using multi-angular, multispectral aerial imagery, (ii) to predict physiological parameters (Chl, nitrogen, nitrogen balance index, percentage of canopy gaps and yield), and (iii) to follow seasonal changes of grapevine physiology in relation to soil management using UAS.

Materials and Methods

1. Study site

Studies were conducted in a commercial vineyard located along the Moselle River in Grevenmacher/Luxembourg (49.69° N, 6.45° E, Figure 1). The vertical shoot positioning trained *Vitis vinifera* L. cv. Pinot blanc vineyard (1.087 ha) was planted on a 125 AA rootstock in 1992. The distance between the rows is 2 m and between single plants 1.2 m. The experimental vineyard is east exposed with an inclination of around 20% and a west-east orientation of the rows.

Standard vineyard management was applied across the whole experimental vineyard in relation to canopy treatment and crop protection treatment.

2. Soil management strategies

Four soil management strategies were realized using a randomized block design, consisting of four

replicates (plots) of five rows each (Figure 1). Soil management strategies were:

- multi-species cover crop mixture, commercial name “Wolff mixture”;
- natural greening;
- summer soil tillage with rotating harrow and winter greening;
- natural greening with disturbance in dry conditions.

Prior to the start of the investigations, all rows had been covered by natural greening for several years. In spring 2010, this natural greening layer was destroyed by tillage in the strategies (1) and (3).

At the beginning of the trial, the multi-species cover crop mixture “Wolff mixture” (Barenbrug Luxembourg SA, Diekirch, Luxembourg) consisting of *Vicia* sp., *Trifolium* spp., *Phacelia* sp., *Onobrychis* sp., *Melilotus* sp., *Medicago* spp. and further herbs was sown in the soil management strategy (1). In this soil management strategy the greening plants were not mulched at all but rolled 3 times per season. Natural greening plants (mainly grass) in soil management strategy (2) were mulched 3 to 4 times per season. In soil management strategy (3) the soil was kept open between April and August using a rotary harrow. In both years, a winter greening mixture consisting of *Vicia* sp., *Lolium* sp., *Trifolium* sp., *Raphanus* sp. and *Malva* sp. was sown in August and plowed in April. The greening layer in soil management strategy (4) was disturbed by rotary harrow in May or June in both years.

3. Field sampling and analysis

All field parameters were assessed for the central row of five rows in plots of 12 plants in the lower area of the experimental vineyard. In both years, canopy morphology (leaf layer number - LLN - and the percentage of gaps in the canopy - PG) was evaluated at BBCH 81 (Lorenz *et al.* 1995) using a modified version of the Point Quadrat Analysis (PQA) protocol of Smart and Robinson (1991). Here, PQA was realized at 1.5 m height above the ground, representing approximately the middle of the canopy (instead of the cluster-zone as proposed by Smart and Robinson (1991)). To this end, a rod was inserted into the canopy every 10 cm from the south side of the canopy. All contacts of the rod were recorded distinguishing between leaves (L) and gaps (G) on 48 insertion points per plot.

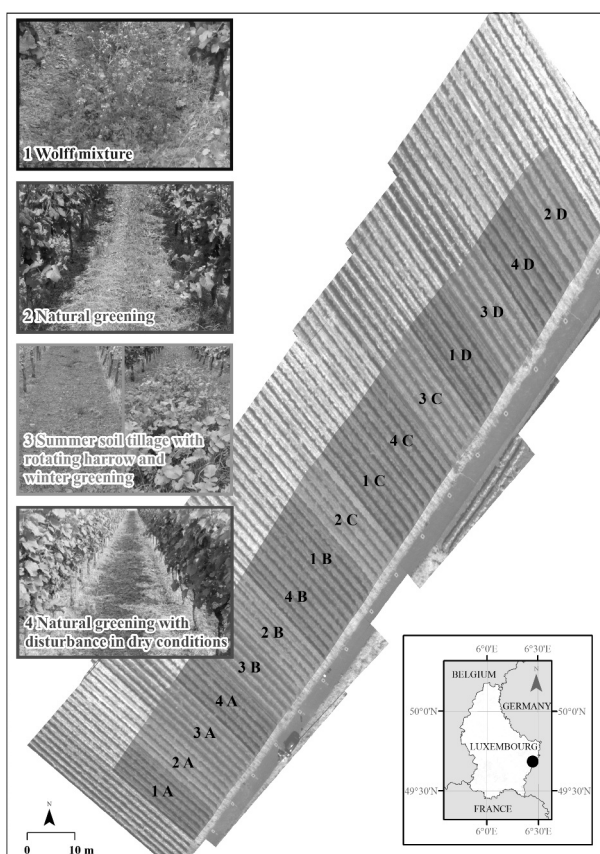


Figure 1 – Plot plan of soil management strategies (1-4) and replicates (A-D) at the experimental vineyard in Grevenmacher/Luxembourg.

Leaf Chl content was determined using Dualex® equipment (Force-A, Paris, France) in both years four times between fruit set and harvest. Measurements were performed on 40 leaves per plot collected in the upper canopy on 09/06/2011 (2011 – I), 12/07/2011 (2011 – II), 17/08/2011 (2011 – III), 21/09/2011 (2011 – IV), 21/06/2012 (2012 – I), 18/07/2012 (2012 – II), 20/08/2012 (2012 – III) and 26/09/2012 (2012 – IV) and transported in cooling boxes to the laboratory. Here, Dualex measurements were performed. Thereafter, leaf discs were punched from the same leaves, dried at 60°C for 24 hours and ground. N contents were quantified with a TruSpec elemental analyser (LECO Corporation, St. Joseph, MI, USA) (Mayer *et al.* 2013). Additionally, the nitrogen balance index (NBI) was assessed by the ratio of the Dualex®-derived Chl and flavonol content (Martinon *et al.* 2010).

Plots were harvested separately on 20/09/2011 and 10/10/2012 and total yield per plant determined. Pruning wood weight per plant was measured on 30/11/2011 and 21/11/2012.

4. UAS imagery

4.1 UAS image acquisition

Flights were carried out with a md4-1000 quadcopter (microdrones GmbH, Siegen, Germany), and images of the experimental vineyard were taken once in 2011 and four times throughout the season in 2012 (Table 1). Multispectral imagery was obtained with a Mini-MCA6 multispectral camera array (Tetracam Inc., Chatsworth, CA, USA; image size of 1280 x 1024 pixels) at 10-bit radiometric resolution, equipped with 10-nm FWHM filters with a central wavelength (CWL) of 530, 550, 570, 670, 700, 900 nm. The camera has been described in detail by Kelcey and Lucieer (2012) but had undergone a rear-to-front filter change at the producer's laboratory at the end of 2011.

In 2011, three camera pointing angles were applied (nadir, 45° off-nadir both on illuminated and shaded parts of the vine rows). Nadir and 45° off-nadir only on illuminated sides were realized in 2012. The flight altitude was 70 m and resulted in a pixel resolution of about 4 cm x 4 cm. Weather was clear and sunny with low winds on each individual flight date (Table 1). Ground control points highlighted each assayed row, and reference grey-scale panels were placed for radiometric calibration purposes.

4.2 Image pre-processing

Image pre-processing included conversion of raw values band-to-band alignment. The six individual camera's images were aligned to a principal plane by x-, y-translation, rotation and scaling using PixelWrench2 (Tetracam Inc. 2003-2014), followed by vignetting correction and combined to multispectral images with in-house developed software. ERDAS Imagine 2014 and ENVI software was used for all further processing.

To derive commonly applied vegetation indices (Table 2) of reflectance data used in similar studies (Zarco-Tejada *et al.* 2004, Zarco-Tejada *et al.* 2013a), grey values were converted to reflectance data by an empirical line correction (ELC) utilising laboratory-derived reflectance measurement of invariant reference panels following Roberts *et al.* (1986) and Smith and Milton (1999). The reference consisted of four painted wooden boards of the colours white, light grey, dark grey and black (Figure 2). Spectral measurements were conducted with a FieldSpec Pro spectroradiometer (ASD Inc., Boulder, CO, USA).

In accordance to field sampling, all assayed rows were digitised at the bottom part of the vineyard to retrieve the relevant canopy spectral values of the upper leaf layer (the sampling horizon) in the oblique images and for the top canopy layer for the

Table 1 – Weather conditions and grape phenological stages at UAS flights (Lorenz *et al.* 1995)

Date	UTC	Weather conditions (temperature, relative humidity RH, solar irradiation)	BBCH stage
17/08/11	10:00h 10:30h	23.3°C, 58% RH, 788 Wh/m ²	81 Beginning of ripening
03/07/12	13:05h 13:15h	24.3°C, 47% RH, 716 Wh/m ²	71 Fruit set
23/07/12	11:30h 12:30h	23.3 - 24°C, 45% RH, 740 Wh/m ²	77-79 Berries touching
03/09/12	10:00h 11:12h	21.8 - 22.6°C, 53 - 60% RH, 750 - 700 Wh/m ²	85 Softening of berries
30/09/12	12:23h 13:05h	16.5 - 17.2°C, 51 - 58% RH, 748 - 780 Wh/m ²	89 Berries ripe for harvest

UTC: coordinated universal time

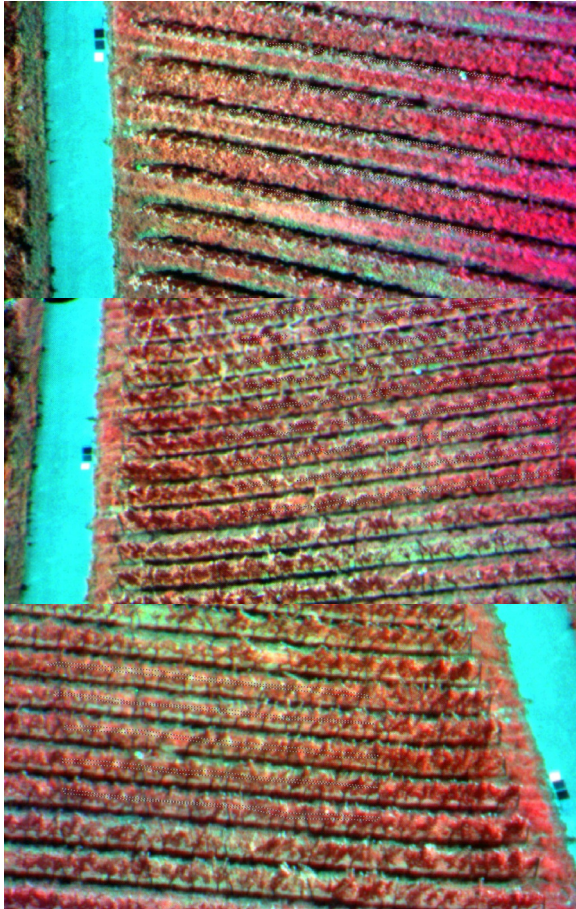


Figure 2 – UAS imagery with nadir (top), 45° off-nadir on illuminated (middle), and 45° off-nadir on shaded grapevine canopy and sampling zones (dashed white polygons) used for statistical analysis.

nadir images using ERDAS Imagine (Figure 2). Canopy gaps were generally avoided.

Vegetation indices (Table 2) were calculated and image statistics derived for the digitised sampling zones (mean, minimum, maximum and standard deviation).

Similarly, the images obtained for the multiple flight dates in 2012 were normalized for radiometric and illumination differences by ELC using *in-situ*-derived reflectances from the reference panels mentioned previously, and reflectances for the sampling horizon were retrieved for the assayed rows accordingly. For the maps of seasonal changes of Chl, non-vineyard canopy pixels needed to be masked out. A binary map was derived by a principal component analysis of the image bands followed by an unsupervised classification to separate only grapevine canopies for further analysis. The Iterative Self-Organizing

Table 2 – Common vegetation indices for retrieving physiological variables used in this study

Vegetation index	Formulation	Author	Application
Simple Ratio Index	$SR = R_{nir}/R_{red}$	Jordan 1969	Structural index, plant vitality
Normalized Difference Vegetation Index	$NDVI = (R_{nir} - R_{red}) / (R_{nir} + R_{red})$	Rouse <i>et al.</i> 1974	Structural index, plant vitality
Transformed Chlorophyll Absorption in Reflectance Index	$TCARI = 3 [(R_{700} - R_{670}) - 0.2 (R_{700} - R_{550}) (R_{700}/R_{670})]$	Haboudane <i>et al.</i> 2002	Chl index, less influence of LAI
Optimized Soil-Adjusted Vegetation Index	$OSAVI = (1 + 0.16) (R_{nir} - R_{red}) / (R_{nir} + R_{red} + 0.16)$	Rondeaux <i>et al.</i> 1996, Haboudane <i>et al.</i> 2002	Chl index, less sensitive to soil background
Photochemical Reflectance Index	$PRI = (R_{531} - R_{570}) / (R_{531} + R_{570})$	Gamon <i>et al.</i> 1997	Carotenoids/Chl index, Chl fluorescence, radiation use efficiency, water stress
Renormalized Difference Vegetation Index	$RdVI = (R_{nir} - R_{red}) / (R_{nir} + R_{red})^{0.5}$	Roujean and Breon 1995	Structural index related to fAPAR
Red Edge Ratio Index	$RE = R_{700}/R_{670}$	Part of TCARI; Zarco-Tejada <i>et al.</i> 2013a, Zarco-Tejada 2013b	Chl content

Table 3 – Field parameters assessed in the experimental vineyard for 2011 (arithmetic mean \pm standard deviation in parentheses)

Parameter	Soil		Soil		Soil	
	Management Strategy 1: “Wolff mixture”	Management Strategy 2: Natural greening	Management Strategy 3: Winter greening	Management Strategy 4: Natural greening with disturbance	Management Strategy 3: Winter greening	Management Strategy 4: Natural greening with disturbance
LLN	1.17 (± 0.31)	1.11 (± 0.19)	1.79 (± 0.3)	1.64 (± 0.37)	1.79 (± 0.3)	1.64 (± 0.37)
PG (%)	33.37 (± 11.5)	35.50 (± 6.81)	18.00 (± 9.52)	23.00 (± 10.89)	18.00 (± 9.52)	23.00 (± 10.89)
Chlorophyll (Duallex units)	21.61 (± 3.26)	19.61 (± 2.4)	26.09 (± 2.52)	21.41 (± 1.58)	26.09 (± 2.52)	21.41 (± 1.58)
Yield per vine (kg)	2.63 (± 0.29)	2.69 (± 0.67)	4.22 (± 0.38)	3.03 (± 0.83)	4.22 (± 0.38)	3.03 (± 0.83)
Pruning weight per plant (kg)	0.45 (± 0.13)	0.39 (± 0.10)	0.57 (± 0.16)	0.51 (± 0.13)	0.57 (± 0.16)	0.51 (± 0.13)
N (% dry weight, sampling date I, 21.09.2011)	1.80 (± 0.22)	1.77 (± 0.27)	2.09 (± 0.14)	1.82 (± 0.21)	2.09 (± 0.14)	1.82 (± 0.21)

Data Analysis Technique (ISODATA) algorithm (Memarsadeghi *et al.* 2007, Intergraph Corporation 2013) was used for the unsupervised classification with an input of 10 classes. The resulting classes were analysed and only classes that represent grapevine canopy pixels were retained and recoded into a binary map indicating only vine canopy.

It is important to note that image acquisition could not always be carried out at the same dates when field parameters were assessed due to weather or other reasons (availability of UAS and sensors, pilot) leading to a time-shift between the respective data sets.

4.3 Statistical data analysis

Statistical analysis on the 2011 and 2012 data sets was carried out a) to analyse the correlation structure among the variables, b) to assess the impact of the different soil management strategies on canopy reflectance, and c) to establish quantitative prediction models for a spatial assessment of selected plant physiological properties based on the measured reflectance data. The correlation structure among the measured reference data and band values data of 2011 was visualised using a heat map of pairwise Pearson’s correlation coefficients of all properties, considering all flight directions and physiological variables.

Differences among canopy reflectance caused by the different soil management strategies were analysed using both visual inspection (box-plots) and linear discriminant analysis (LDA). The LDA was carried out for each viewing direction, with soil management as grouping factor and the vegetation indices as explanatory variables. The following indices were used: SR, NDVI, TCARI, OSAVI, TCARI/OSAVI, PRI, RE, and RDVI (see Table 2).

The quantification of selected vegetation properties (Chl and N content, leaf layer number LLN, percentage of gaps PG in the upper canopy and yield) using grey value (i.e. DN, digital number) data was accomplished using forward stepwise multiple regression analysis. Different regression models were calibrated for the 2011 and 2012 data sets: the major aim of the 2011 analyses was to understand the impact of the viewing direction on plant property estimations and to derive the most appropriate wavelengths in doing so. To this end, the combined reflectance data set, including the data from all viewing directions, was included in the stepwise regression models. The intention of

the 2012 analysis was to calibrate global regression models for estimating key biophysical plant parameters and to exemplarily compare the resulting spatial estimations of Chl content. In this stepwise regression only data of the illuminated 45° viewing direction were considered since the performance of these data was better compared to the nadir and shaded 45° viewing direction. All regression models were internally validated using leave-one-out (LOO) cross-validation. The statistical analysis was carried out using the R software package.

Results

1. Field data results of 2011

The results of the field assessments in the season 2011 are summarised in table 3. Soil management strategy (3) (winter greening and soil tillage in summer) showed highest Chl and N contents, more leaves in the upper canopy, as well as the highest pruning weight and yield per plant.

2. Spectral separability of soil management strategies observed by different viewing angles (2011 data)

The score plot of the PC 1 and 2 (Figure 3) demonstrates a higher variability of reflectance values depicted by the oblique viewing geometry of illuminated canopy parts (red) compared to the

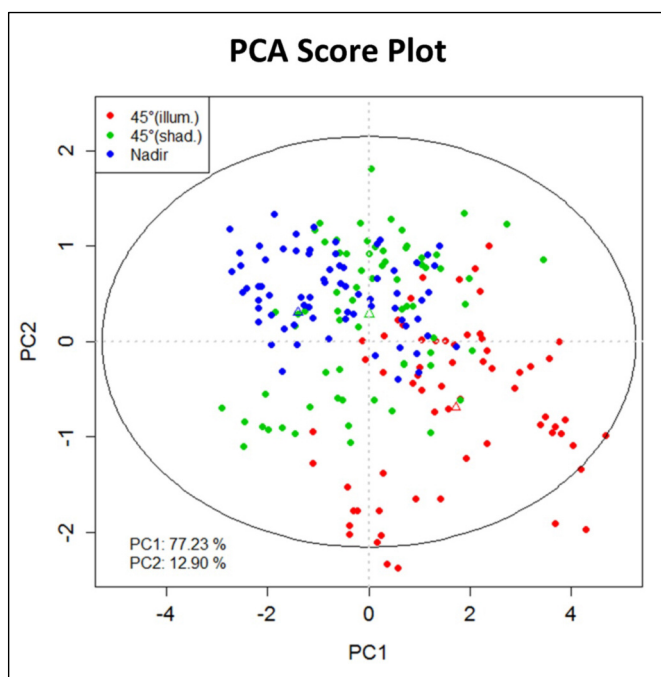


Figure 3 – Plot of the principal component 1 and 2 for all rows and nadir and oblique viewing geometries.

narrower ranges of nadir values (blue) and shaded canopy parts (green).

Figure 4 shows box-plots of the different vegetation indices (SR, NDVI, PRI, RDVI, TCARI, and OSAVI) versus the soil management strategy for the three considered viewing geometries (nadir, forward/illuminated, backward/shaded grapevine sides). The central tendencies of all these vegetation indices show remarkable differences between the four different soil management systems for the oblique viewing directions and especially for the 45°-illuminated direction (SR, NDVI, RDVI, OSAVI), whereas for the nadir direction the soil management systems show very similar means and cannot be separated from each other.

This was confirmed by linear discriminant analysis that was carried out for each viewing direction, with soil management as grouping factor and the vegetation indices as explanatory variables. Table 4 summarises the (cross-validated) total accuracies of the respective models and the standardized discriminant coefficients of the first two functions that represent the contribution of a variable to the discriminant function in the context of the other predictor variables in the model. The total accuracy of the model that is based on the nadir viewing direction is 48.75%, whereas in both oblique viewing directions >70% of the data could be correctly classified.

The discriminant coefficients in table 4 further show that the vegetation indices TCARI, OSAVI, TCARI/OSAVI, RDVI and to a lower extent NDVI mostly contribute to the discrimination, especially for the illuminated canopies.

3. Ability to predict physiological parameters and yield for grapevine using different viewing angles (2011 data)

Figure 5 shows a heat map to depict the correlation among the measured plant parameters in the vegetation period 2011. Plant parameters from all dates were included in the analysis. There is a group of variables that are positively correlated (Chl, N, LLN, yield). The variable PG is negatively correlated with this group. From the remote sensing perspective, among these variables, the Chl content is the most interesting one, since chlorophyll can be predicted from multispectral remote sensing data and may be linked to yield. The heat map also illustrates the increasing correlation between Chl and yield with image acquisition dates progressing to the end of season.

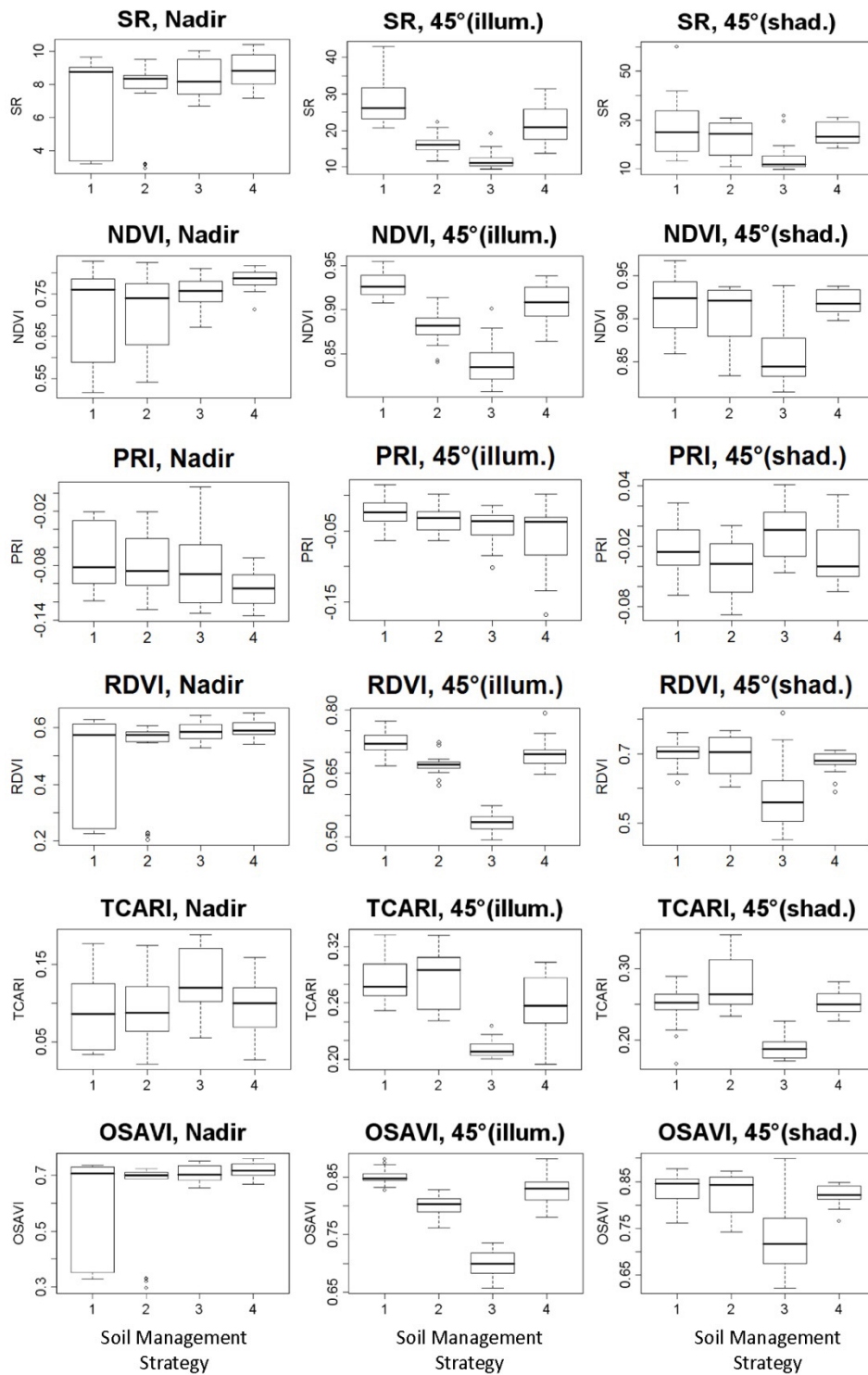


Figure 4 – Box-plots of different vegetation indices versus soil management strategies 1- 4 (x-axis) for the viewing geometries nadir, illuminated and shaded grapevine sides (black line: median, boxes:

Table 4 – Standardized discriminant coefficients of the first two discriminant functions, proportion of trace and cross-validated total accuracies for LDA models for different viewing directions (n=215)

	Nadir		45°(illum.)		45°(shad.)	
	LD1	LD2	LD1	LD2	LD1	LD2
SR	-5.77	-1.35	0.67	3.74	3.40	-0.56
NDVI	0.45	0.93	5.19	0.66	0.65	-0.83
PRI	1.86	0.01	-0.19	0.27	-0.00	0.27
RE	-0.96	3.16	0.05	-1.23	-3.15	2.21
TCARI	5.74	-8.94	17.40	20.72	4.37	5.32
OSAVI	-1.32	-12.22	-28.80	-15.64	-5.14	-11.66
TCARI/OSAVI	-3.82	4.85	-14.02	-15.68	-3.70	-4.42
RDVI	6.13	15.60	11.17	2.83	0.38	9.69
Prop. of trace	0.69	0.25	0.89	0.08	0.86	0.08
Total acc. (CV)	48.75%		70.77%		70.25%	

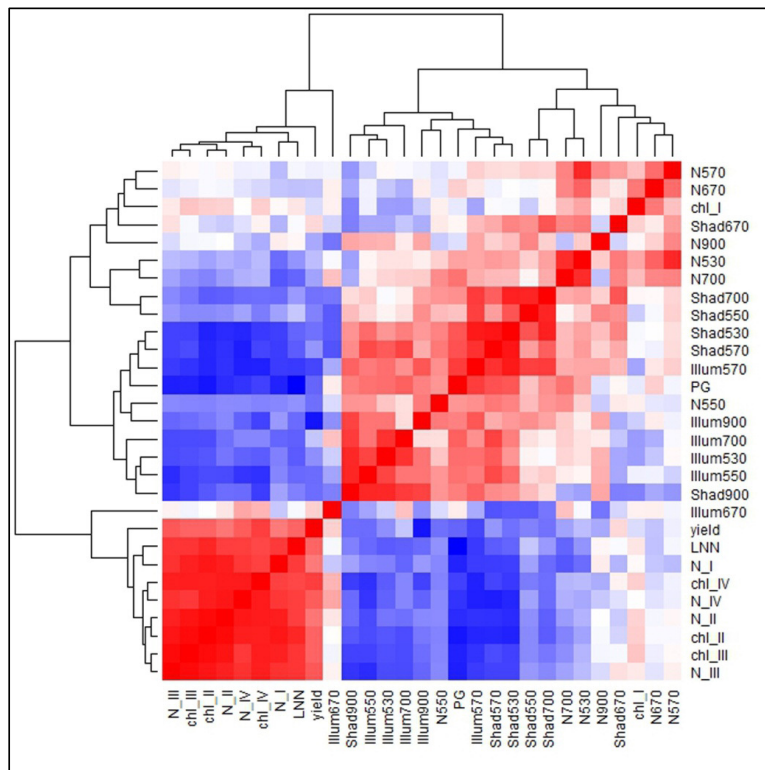


Figure 5 – Heat map of in-situ measured physiological variables in 2011 (red: high correlation, blue: low correlation, N: nadir, Shad: shaded, Illum: illuminated, I-IV are measurement dates of in-situ sampling from beginning of berry development to harvest (I: BBCH 71, II: BBCH 77, III: BBCH 85 and IV: BBCH 89), chl_ : chlorophyll, N_ : nitrogen, LNN: leaf layer number, PG: percentage of gaps).

Table 5 – Derived regression models for predicting measured variables of 2011 field samples for each viewing geometry
(X: Band, Significance codes: 0 ‘*’, 0.001 ‘**’, 0.01 ‘*’, 0.05 ‘.’, 0.1 ‘’)**

Chlorophyll	Nadir	45°(illum.)	45°(shad.)
Intercept	549.101	541.1043	529.7517
X ₅₃₀			0.000246 ***
X ₅₅₀	0.0403 *	0.00223 **	
X ₅₇₀		0.00318 **	
X ₇₀₀		0.05216 .	0.043850 *
N	16	14	13
R ² _{cv}	0.26	0.85	0.76
RMSE _{cv}	34.64	17.21	19.92

N	Nadir	45°(illum.)	45°(shad.)
Intercept	3.6251	3.39543	3.7748189
X ₅₃₀			9.93E-05 ***
X ₅₅₀	0.083350 .	0.000884 ***	
X ₅₇₀		0.004124 **	
X ₇₀₀		0.029463 *	0.00338 **
N	16	14	13
R ² _{cv}	0.24	0.85	0.76
RMSE _{cv}	0.184	0.11	0.126

PG	Nadir	45°(illum.)	45°(shad.)
Intercept	-30.1074	-25.22294	-31.609778
X ₅₃₀		0.017161 *	
X ₅₅₀	0.0184 *	0.151129	2.37E-06 ***
X ₅₇₀		0.000276 ***	
X ₆₇₀		0.002361 **	
N	16	14	13
R ² _{cv}	0.4	0.66	0.84
RMSE _{cv}	6.81	4.89	2.97

Yield	Nadir	45°(illum.)	45°(shad.)
Intercept	10.563235	6.28664	3.540241
X ₅₃₀		0.029139 *	
X ₅₅₀	0.010237 *	0.056265 .	0.185868
X ₅₇₀		0.095864 .	
X ₇₀₀		0.024746 *	0.000964 ***
X ₆₇₀			0.001972 **
X ₉₀₀	0.055355 .	0.000236 ***	
N	16	14	13
R ² _{cv}	0.51	0.84	0.68
RMSE _{cv}	0.57	0.34	0.46

First, the influence of the different viewing directions on the quantitative predictions of four selected plant properties (Chl, N, PG, and yield) was tested. To this end, stepwise linear regression models were computed for each viewing direction to identify the most relevant wavelengths for estimating plant properties, using the Akaike information criterion (AIC). Validation was accomplished by LOO cross-validation (Table 5).

Table 5 demonstrates that for a given plant property different models were identified for the different viewing directions using the stepwise linear regression approach. In general, best results for each plant characteristics were obtained using the reflectance data from the oblique viewing geometries. Beside PG, the 45° sun-illuminated canopy parts showed higher coefficients of determination than the shaded sides. The cross-validated R² values in our case range from 0.66

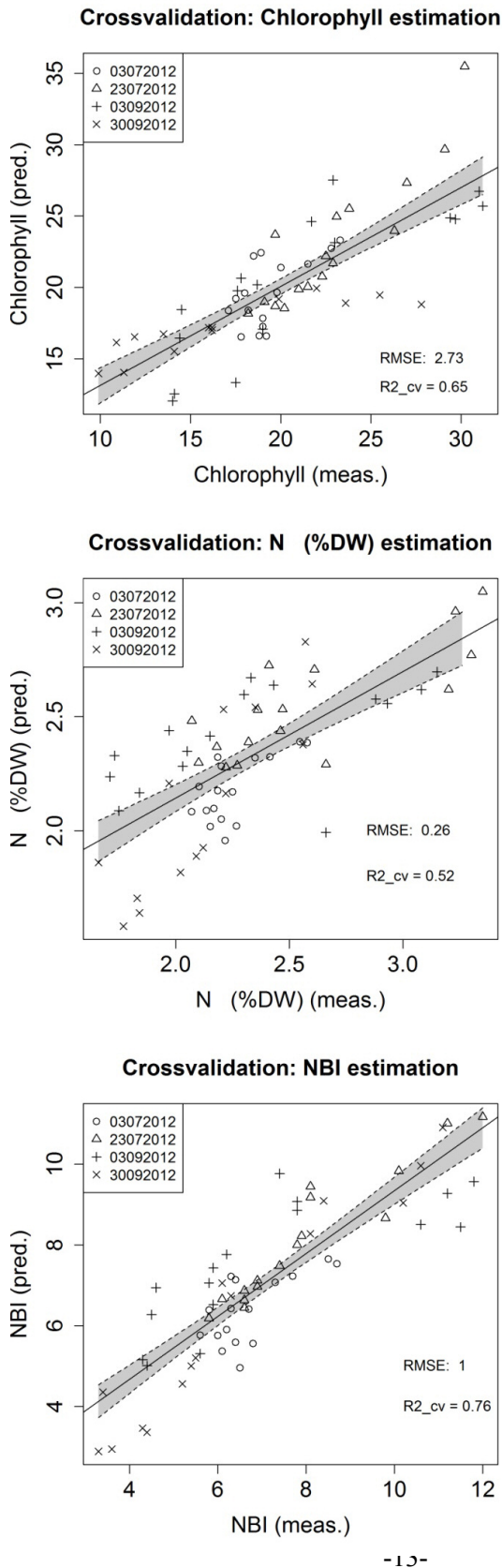


Figure 6 – Cross-validated regression models and model coefficients for Chl, N, and NBI content for 2012.

(PG) to 0.85 (Chl, N). In contrast, spectral signatures taken from nadir did not, except for yield, lead to reliable quantitative estimations of the plant characteristics.

Predicting seasonal changes in grapevine physiological parameters (2012 data)

As in the previous year, the best separability was obtained from oblique imagery of the illuminated grapevine parts, therefore only these images were further processed for the 2012 data. Regression models were computed for Chl, N, and NBI including all dates. Compared to individual stepwise regression models, for each date in 2011 with a $R^2_{cv} > 0.8$, the global predictive models' R^2_{cv} in 2012 were lower but, except for N with $R^2_{cv} = 0.52$, still ranged from $R^2_{cv} = 0.65$ for Chl and $R^2_{cv} = 0.76$ for NBI (Figure 6). Table 6 lists the associated model coefficients which include the nIR band (900 nm) and the red edge (700 nm) as highly significant (p value < 0) for all parameters models, and for Chl also the Chl peak near 550 nm.

Based on the retrieved regression models, seasonal Chl values were spatially estimated for each vine row for each image acquisition date (Figure 7). For visualisation purposes, only replicate A has been selected, all other replicates do show similar trends though (Figure 8). The Chl content shows clear differences depending on the BBCH stages and retrieved reflectances.

The seasonal course of predicted canopy Chl illustrates that soil management strategy (3) with winter greening and summer soil tillage, showed except for early summer, the highest values on all dates followed by the “Wolff mixture” (strategy (1)). For the natural greening and natural greening with disturbance during dry conditions, late summer/early autumn date Chl values diminish faster than for the other soil management strategies.

Measured Chl(Dualex) values for replicate A-D confirm these results (Figure 8). The Chl values are generally highest and persist at higher levels even for September (DOY 270) compared to other soil management strategies, with respective correlation coefficient between measured and predicted Chl values being $R = 0.84$ for soil management strategy (1), $R = 0.84$ for (2), $R = 0.94$ for (3) and $R = 0.99$ for (4).

Discussion

Among others, Gil-Perez *et al.* (2010), Tardaguila *et al.* (2011) and Arnó *et al.* (2012) have recently

Table 6 – Model coefficients for cross-validated regressions models for Chl, N and NBI in 2012 of Figure 6 (Significance codes: 0 ‘*’, 0.001 ‘**’, 0.01 ‘*’, 0.05 ‘.’, 0.1 ‘.’)**

Coefficients	Estimates	Standard Error (SE)	t value	Pr (> t)	Sign.
Chl					
Intercept	31.9502625	1.8207056	17.548	< 2E-16	***
X ₉₀₀	0.0032500	0.0002935	11.074	9.96E-16	***
X ₇₀₀	-0.0182065	0.0030136	-6.041	1.30E-07	***
X ₅₃₀	0.0125341	0.0043080	2.910	0.00518	**
X ₅₅₀	-0.0117183	0.0021620	-5.420	1.31E-06	***
Multiple R ² 0.7068	Adjusted R ² 0.6859	Residual SE 2.822	F-Statistic 38.76 on 4 and 56 DF	p-value 2.493E-14	
N					
Intercept	2.073E+00	2.059E-01	10.067	3.59E-14	***
X ₉₀₀	3.166E-04	4.767E-05	6.642	3.50E-07	***
X ₇₀₀	-1.423E-03	2.528E-04	-5.632	5.99E-07	***
X ₅₃₀	5.286E-04	2.142E-04	2.467	0.0167	*
X ₆₇₀	9.773E-04	4.655E-04	2.100	0.0403	*
Multiple R ² 0.5758	Adjusted R ² 0.5455	Residual SE 0.271	F-Statistic 19 on 4 and 56 DF	p-value 6.398E-10	
NBI					
Intercept	5.4260802	0.6973468	7.781	1.43E-10	***
X ₉₀₀	0.0020961	0.0001669	12.557	< 2E-16	***
X ₇₀₀	-0.0074283	0.0006788	-10.943	9.91E-16	***
X ₆₇₀	0.0053489	0.0012923	4.139	0.000114	***
Multiple R ² 0.7895	Adjusted R ² 0.7786	Residual SE 1.026	F-Statistic 72.52 on 3 and 58 DF	p-value 2.2E-16	

pointed out the great importance of soil fertility, soil depth, as well as the mineral petiole concentration for producing high quality wines.

In the present work, DN_s and reflectances of four soil management strategies were analysed by nadir and oblique viewing geometries. We were able to show that different soil management strategies result in differences in the Vis/nIR spectral range during the growing season and may well be separated by a multispectral camera. We found that compared to nadir images, oblique images significantly boosted the spectral separation of grapevine canopy reflectance of different soil management strategies (Figure 3). This is in

accordance with the findings of Kempeneers *et al.* (2008) and Meggio *et al.* (2008), who successfully modelled Chl concentration from hyperspectral reflectances perpendicular to the solar plane by inverting a 3D ray tracing canopy model. Signal contamination by spurious soil pixels possibly still remaining in the polygons retrieving the image spectral signal did not seem to affect the statistical separation. First, as arithmetic means were computed for each row, potential soil signal effects are supposed to become negligible. Also, one would expect the results for the oblique viewing geometries to be more affected by spurious soil pixels and should have performed worse as more

soil signal is potentially included in the area. This was not the case.

The multispectral images obtained from a UAS for August 2011 showed that the canopy reflectance of illuminated canopy fractions has a larger variance in the PC space of 1st and 2nd principal component (PC) than the nadir image (Figure 2). The shaded canopy parts, however, are rather a mixture of these two.

Comparing the performance of common vegetation indices (VI) listed in table 2, we were able to confirm the higher suitability of oblique viewing angles on illuminated canopy (Table 4). Hyperspectral VIs such as OSAVI, TCARI, TCARI/OSAVI and PRI have been described as being sensitive to Chl a+b changes for *Vitis vinifera* L. leaves and canopies (Zarco-Tejada *et al.* 2005, Gil-Perez *et al.* 2010, Martín *et al.* 2007, Zarco-Tejada *et al.* 2005, Zarco-Tejada *et al.* 2013a), and indeed OSAVI, TCARI and TCARI/OSAVI were able to precisely separate the soil management strategies (Table 4), separability being strongest for oblique viewing angles on illuminated canopies. Only poor discriminant power had been found for PRI and RE which can also be inferred from Figure 4. Among the more simple VIs and oblique viewing angles with the sun positioned behind the observer, the RDVI and NDVI also distinguish among soil management strategies. Hall *et al.* (2011b) enhanced the analysis of shaded canopies compared to the sunny sides by normalisation using a shadow fraction derived from multiple viewing geometries.

The second objective in this study was to determine the most appropriate viewing geometry for predicting physiological and canopy parameters, where again best results (Table 5) were obtained using multispectral reflectances of oblique viewing geometries for illuminated canopies for N and Chl (both R^2_{cv} 0.85), and yield (R^2_{cv} 0.84). For PG in the upper canopy, however, the shaded canopy part was better suited for the estimation (R^2_{cv} 0.84). We think the better performance of oblique viewing angles compared to nadir imagery is due to seeing a greater part of the vertically-oriented grapevine canopy, representing the sampling horizon for field data.

Hall *et al.* (2011a) observed changes in correlation direction between canopy and fruit composition and yield in relation with the time point of image acquisition after the budbreak: in the early BBCH stages, the correlation was negative, converting to positive later in the season. Similar results were

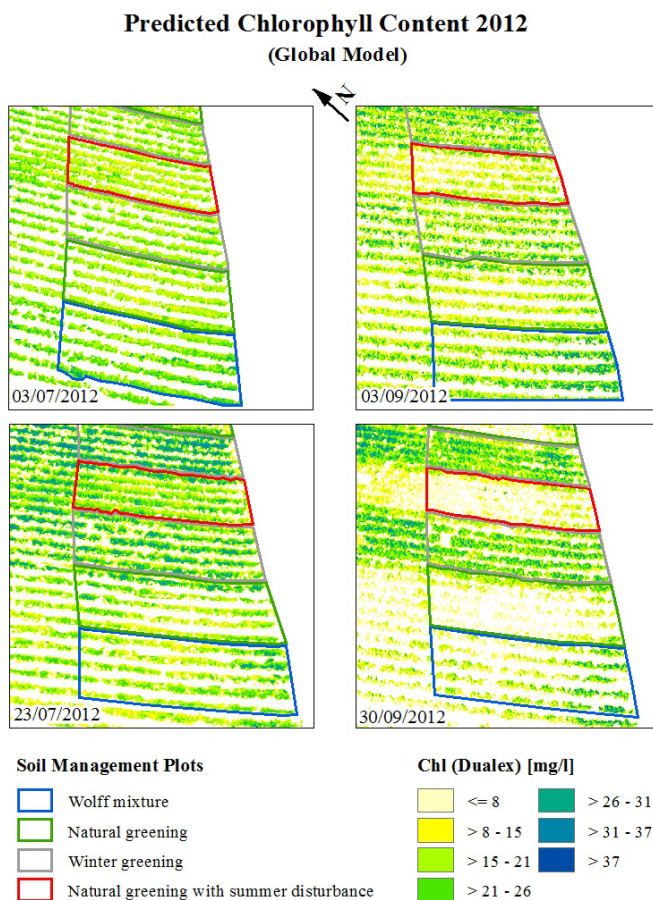


Figure 7 – Chlorophyll estimation for image acquisition dates based on global regression model of Chl and reflectances 2012, replicate A.

found for relationships between Chl and yield for the 2011 data (Figure 4), where early Chl (chl_I) values at fruit set were negatively correlated with yield. Hall *et al.* (2011a) therefore rightly point out the importance of selecting appropriate image acquisition dates.

In spite of careful pixel selection using manual digitising and unsupervised classification, a possible signal contamination by spurious soil pixels could not be fully excluded in the statistical analysis. However, as arithmetic means were computed for each row, potential soil signal effects are suppressed. If they were not, the results for the oblique viewing geometries should have been more affected and expected to perform worse as more soil signal is potentially included in the area, which was not the case. In fact, the optimal retrieval of leaf chemical components was achieved from the oblique viewing directions.

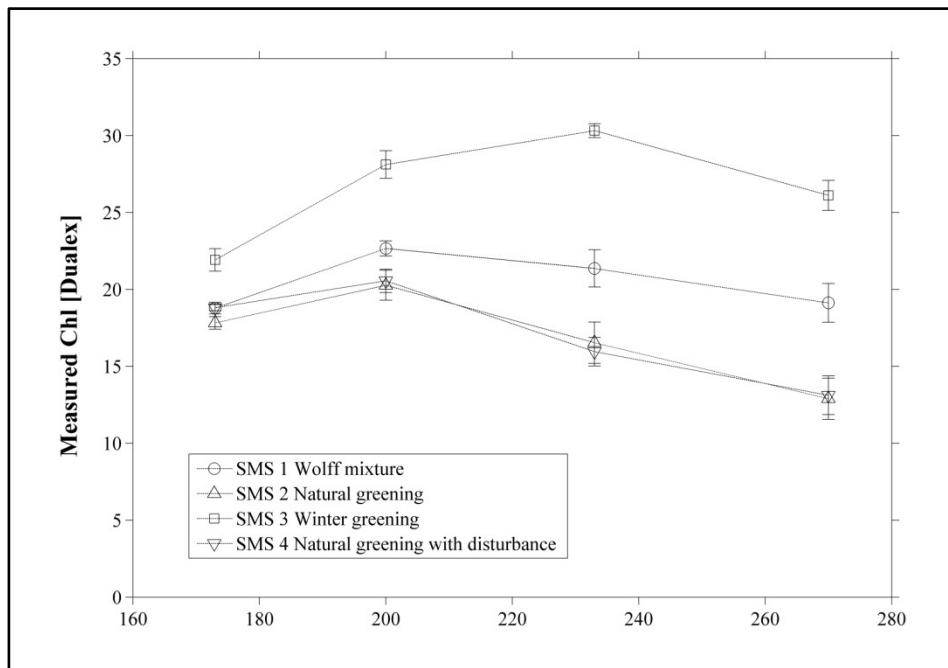


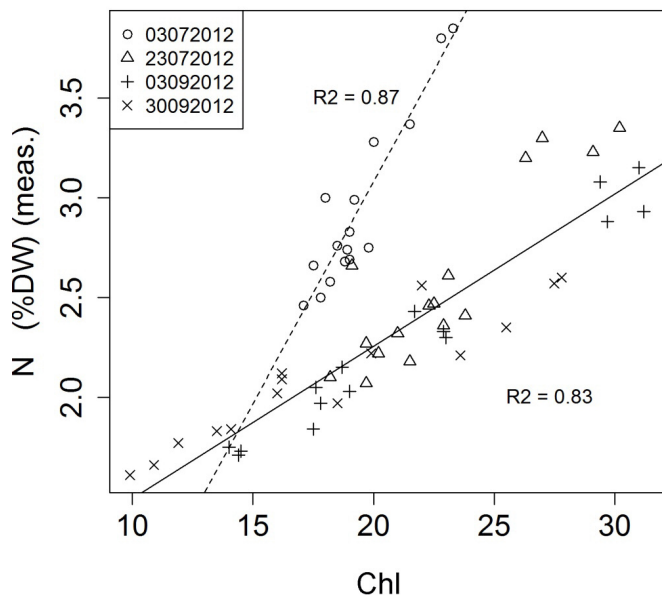
Figure 8 – Mean seasonal course and standard deviation of measured Chl (Dualex) across all replicates for 2012.

The global regression models estimating Chl and NBI content throughout the season of 2012 showed slightly lower R^2_{cv} values (0.65 and 0.76, respectively) than in 2011 (Chl and N $R^2_{cv} = 0.85$), for N even $R^2_{cv} = 0.52$ (Figure 6, Table 4). Generally, the quantification of the N content from spectroscopic data using empirical models is mainly indirect via the positive correlation between N and Chl. In fact, table 5 shows that, apart from the wavelength 550 nm, the stepwise multiple regression selected the same wavelengths (900 nm, 700 nm and 530 nm) for both variables and respective regression coefficients have the same signs. N is positively correlated with the Chl content as it is contained in the Chl pigments (Guyot 1990, Jensen 2007), which is the optically active parameter for remote sensing. Figure 9 shows the linear relationship between N and Chl for the early flight at fruit set ($R^2_{cv} = 0.87$), and the later flight dates in 2012 ($R^2_{cv} = 0.83$). It illustrates that early in the season, the relationship between Chl and N is different than for later development stages, leading to an overall lower R^2_{cv} value of 0.52 for the prediction of N for the whole season. This again consolidates the importance of selecting appropriate BBCH stages for image acquisition. The prediction's accuracy of N therefore increases if the first flight data was subtracted from the 2012 analysis. As Figure 9 additionally shows, the NBI is directly linked to Chl content as it is derived

from the same optical measurement device (i.e. Dualex).

Furthermore, remaining bidirectional reflectance differences between *in-situ* spectral measurements and sensor-viewing and row geometry may add to that effect (Zarco-Tejada *et al.* 2005). Another reason for lower correlations in 2012 compared to 2011 may be attributed to time delay between field parameter derivation and image acquisition (Figure 10). Due either to weather conditions or logistic reasons (e.g. availability of instruments), image acquisition could not always take place at field measurement dates. However, the general progression is nevertheless following the measured Chl course (Figure 10).

The soil management strategy (3) (winter greening) was the most vigorous in terms of Chl values, followed by soil management strategy (1) (“Wolff mixture”) (Figure 8). Figure 8 also shows the greater late summer drop of mean measured Chl for soil management strategy (2) (natural greening) and (4) (natural greening with disturbance). This suggests that grapevine vigour is fostered by lack of competing cover crops. Similar results had been found for more Mediterranean type climate zones (Clarke *et al.* 2006, Tesic *et al.* 2007).



N vs. NBI

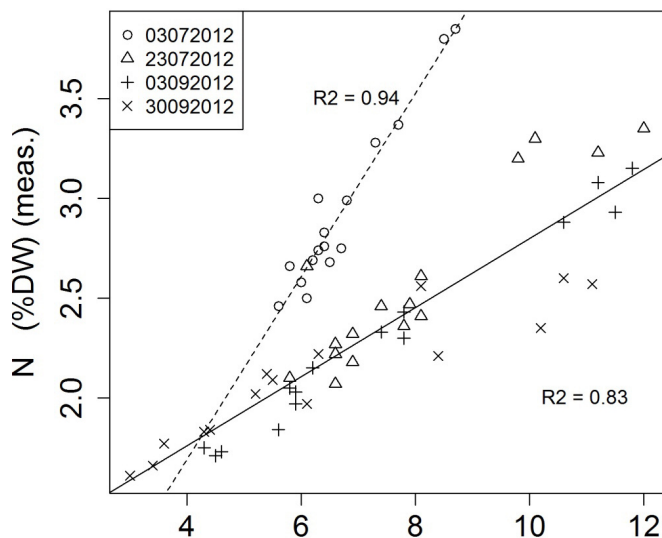


Figure 9 – Plot of Chl (Dualex) versus N (top) and NBI (Dualex) versus N content for the field measurements in 2012.

Conclusion

UAS-based imagery has yet again proven to be a useful tool for rapid spatial information of vineyard vigour and precision viticulture. Soil management strategies affect grapevine vigour and yield in cool climate viticulture and hence allow for targeted vigour steering. Observed differences in vigour may be well depicted by means of multispectral UAS-based remote sensing and are best retrieved by oblique UAS data. In this work, reflectance of the

illuminated parts of the grapevine canopy was most appropriate to distinguish among soil management strategies using oblique UAS data using simple vegetation indices like the NDVI and RDVI. OSAVI, TCARI and TCARI/OSAVI were also well suited to discriminate soil management strategies at angled views. From multiple UAS images taken at specific BBCH stages from fruit set to pre-harvest, reliable regression models could be derived to estimate Chl and NBI and may help to predict yield. Thus, the presented methodology is a valuable tool for precision agriculture application in small areas. Further analyses should include UAS imagery into 3D presentations of the vine row canopy (Corbane *et al.* 2012) to study in more detail viticultural canopy properties and bidirectional reflectance behaviour as has been exerted for PRI in forests (Hall *et al.* 2008, Hilker *et al.* 2008, Hall *et al.* 2011b).

Acknowledgments: The authors would especially like to thank B. Untereiner, S. Contal, C. Walczak, N. Kinlen, J. Koch, R. Mannes, S. Fischer and C. Blum for their help in the experimental vineyards and in the laboratory, the Institut Viti-vinicole (Remich, Luxembourg) for financial support in the frame of the research project “Vitisol” and N. Ben Ghozlen for her support in using the Dualex® device. Monica Perez supported the UAS flight campaigns in 2012. Finally, we would like to thank the anonymous reviewers for helping to enhance the quality of this paper.

References

- Arnó, J., Rosell, J.R., Blanco, R., Ramos, M.C. and Martínez-Casasnovas, J.A., 2012. Spatial variability in grape yield and quality influenced by soil and crop nutrition characteristics. *Precision Agriculture*, **13**, 393-410.
- Baluja, J., Diago, M., Balda, P., Zorer, R., Meggio, F., Morales, F. and Tardaguila, J., 2012. Assessment of vineyard water status variability by thermal and multispectral imagery using an unmanned aerial vehicle (UAV). *Irrigation Science*, **30**, 511-522.
- Berni, J.A.J., Zarco-Tejada, P.J., Sepulcre-Cantó, G., Fereres, E. and Villalobos, F., 2009a. Mapping canopy conductance and CWSI in olive orchards using high resolution thermal remote sensing imagery. *Remote Sensing of Environment*, **113**, 2380-2388.
- Berni, J.A.J., Zarco-Tejada, P.J., Suárez, L. and Fereres, E., 2009b. Thermal and narrowband multispectral remote sensing for vegetation monitoring from an Unmanned Aerial Vehicle. *IEEE Transactions on Geoscience & Remote Sensing*, **47**, 722-738.

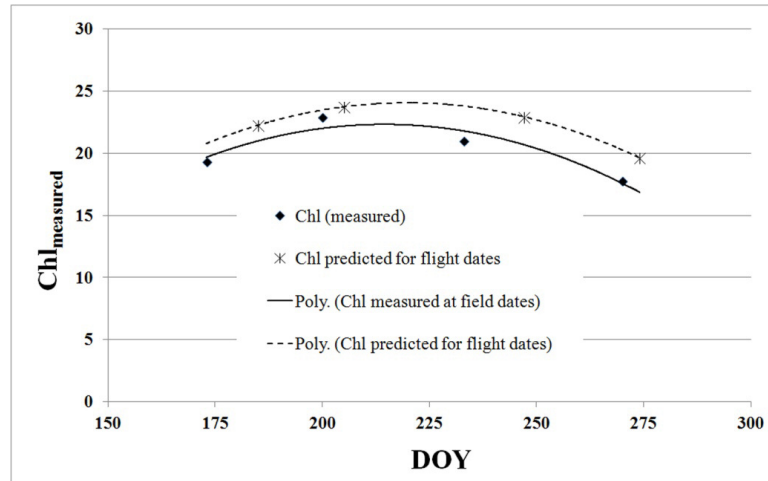


Figure 10 – Time shift between seasonal field Chl measurements (arithmetic mean: black dots) and UAS image acquisition dates (grey asterisks) in 2012.

- Berni, J.A.J., Zarco-Tejada, P.J., Suárez, L., González-Dugo, V. and Fereres, E. 2009c. Remote sensing of vegetation from UAV platforms using lightweight multispectral and thermal imaging sensors. *In: High-Resolution Earth Imaging for Geospatial Information Hannover, Germany*.ed.,6 pages.
- Bramley, R.G.V., Ouzman, J. and Boss, P.K., 2011a. Variation in vine vigour, grape yield and vineyard soils and topography as indicators of variation in the chemical composition of grapes, wine and wine sensory attributes. *Australian Journal of Grape and Wine Research*, **17**, 217-229.
- Bramley, R.G.V., Trought, M.C.T. and Praat, J.P., 2011b. Vineyard variability in Marlborough, New Zealand: characterising variation in vineyard performance and options for the implementation of Precision Viticulture. *Australian Journal of Grape and Wine Research*, **17**, 83-89.
- Clarke, S., Coombes, N., Holloway, J., Hutton, R., Lemerle, D., Loch, A., Meunier, M., Loothfar, R., Rouse, E., Smith, R., Stevens, M., Tesic, D. and Weckert, M., 2006. Floor management systems to reduce vineyard inputs and improve grape quality. Final report. In: N.W.G.I. Centre (ed.), *Grape and Wine Research and Development Corporation*. National Wine & Grape Industry Centre, Wagga Wagga.
- Corbane, C., Jacob, F., Raclot, D., Albergel, J. and Andrieux, P., 2012. Multitemporal analysis of hydrological soil surface characteristics using aerial photos: A case study on a Mediterranean vineyard. *International Journal of Applied Earth Observation and Geoinformation*, **18**, 356-367.
- Gamon, J.A., Serrano, L. and Surfus, J.S., 1997. The photochemical reflectance index: an optical indicator of photosynthetic radiation use efficiency across species, functional types, and nutrient levels. *Oecologia*, **112**, 492-501.
- Gil-Perez, B., Zarco-Tejada, P.J., Correa-Guimaraes, A., Relea-Gangas, E., Navas-Gracia, L.M., Hernandez-Navarro, S., Sanz-Requena, J.F., Berjon, A. and Martin-Gil, J., 2010. Remote sensing detection of nutrient uptake in vineyards using narrow-band hyperspectral imagery. *Vitis*, **49**, 167-173.
- Guyot, G. 1990. Optical properties of vegetation canopies. In: M.D. Steven, & J.A. Clark (eds.), *Applications of remote sensing in agriculture*. Butterworths, London, 19-43 p.
- Haboudane, D., Miller, J.R., Tremblay, N., Zarco-Tejada, P.J. and Dextraze, L., 2002. Integrated narrow-band vegetation indices for prediction of crop chlorophyll content for application to precision agriculture. *Remote Sensing of Environment*, **81**, 416-426.
- Hall, A., Lamb, D.W., Holzapfel, B.P. and Louis, J.P., 2011a. Within-season temporal variation in correlations between vineyard canopy and winegrape composition and yield. *Precision Agriculture*, **12**, 103-117.
- Hall, A. and Wilson, M.A., 2013. Object-based analysis of grapevine canopy relationships with winegrape composition and yield in two contrasting vineyards using multitemporal high spatial resolution optical remote sensing. *International Journal of Remote Sensing*, **34**, 1772-1797.
- Hall, F.G., Hilker, T. and Coops, N.C., 2011b. PHOTOSYNSAT, photosynthesis from space: Theoretical foundations of a satellite concept and validation from tower and spaceborne data. *Remote Sensing of Environment*, **115**, 1918-1925.

- Hall, F.G., Hilker, T., Coops, N.C., Lyapustin, A., Huemmrich, K.F., Middleton, E., Margolis, H., Drolet, G. and Black, T.A., 2008. Multi-angle remote sensing of forest light use efficiency by observing PRI variation with canopy shadow fraction. *Remote Sensing of Environment*, **112**, 3201-3211.
- Hilker, T., Coops, N.C., Hall, F.G., Black, T.A., Wulder, M.A., Nesic, Z. and Krishnan, P., 2008. Separating physiologically and directionally induced changes in PRI using BRDF models. *Remote Sensing of Environment*, **112**, 2777-2788.
- Huete, A.R. and Jackson, R.D., 1988. Soil and atmosphere influences on the spectra of partial canopies. *Remote Sensing of Environment*, **25**, 89-105.
- Intergraph Corporation, 2013. ERDAS Field Guide™. In. Intergraph Corporation, Huntsville, AL, USA,
- Jackson, D.I. and Lombard, P.B., 1993. Environmental and management practices affecting grape composition and wine quality - A review. *American Journal of Enology and Viticulture*, **44**, 409-430.
- Jensen, J.R., 2007. Remote sensing of the environment. An earth resource perspective. 2nd edition, In: K.C. Clarke, Prentice Hall series in Geographic Information Sciences, Pearson Prentice-Hall, Upper Saddle River, NJ.
- Johnson, L.F., Roczen, D.E., Youkhana, S.K., Nemani, R.R. and Bosch, D.F., 2003. Mapping vineyard leaf area with multispectral satellite imagery. *Computers & Electronics in Agriculture*, **38**, 33.
- Kelcey, J. and Lucieer, A., 2012. Sensor correction of a 6-band multispectral imaging sensor for UAV remote sensing. *Remote Sensing*, **4**, 1462-1493.
- Kempeneers, P., Zarco-Tejada, P.J., North, P.R.J., de Backer, S., Delalieux, S., Sepulcre-Cantó, G., Morales, F., van Aardt, J.A.N., Sagardoy, R., Coppin, P. and Scheunders, P., 2008. Model inversion for chlorophyll estimation in open canopies from hyperspectral imagery. *International Journal of Remote Sensing*, **29**, 5093-5111.
- Lorenz, D.H., Eichhorn, K.W., Bleiholder, H., Klose, R., Meier, U. and Weber, E., 1995. Phenological growth stages of the grapevine, *Vitis vinifera* L. ssp. *vinifera*. Codes and descriptions according to the extended BBCH scale. *Australian Journal of Grape and Wine Research*, **1**, 100-103.
- Martín, P., Zarco-Tejada, P.J., González, M.R. and Berjon, A., 2007. Using hyperspectral remote sensing to map grape quality in 'Tempranillo' vineyards affected by iron deficiency chlorosis. *Vitis*, **46**, 7-14.
- Martinon, V., Fadailli, E.M., Becu, M., Duval, C. and Fumery, J. 2010. Innovative optical sensors for diagnosis, mapping and real-time management of row crops: the use of polyphenolics and fluorescence. In: *ASA, CSSA, and SSSA 2010 International Annual Meetings, 31/10 - 03/11/2010, Long Beach, CA, USA*.ed.,1.
- Mathews, A. and Jensen, J., 2013. Visualizing and quantifying vineyard canopy LAI using an Unmanned Aerial Vehicle (UAV) collected high density Structure from Motion point cloud. *Remote Sensing*, **5**, 2164-2183.
- Mayer, F., Noo, A., Sinnaeve, G., Dardenne, P., Gerin, P.A. and Delfosse, P., 2013. Prediction of the biochemical methane potential (BMP) of maize silages reduced to a powder using NIR spectra from wet and dried samples. In, *NIR 2013 - 16th International Conference on Near Infrared Spectroscopy*34280 La Grande-Motte.
- Meggio, F., Zarco-Tejada, P.J., Miller, J.R., Martin, P., Gonzalez, M.R. and Berjon, A., 2008. Row orientation and viewing geometry effects on row-structured vine crops for chlorophyll content estimation. *Canadian Journal of Remote Sensing*, **34**, 220-234.
- Meggio, F., Zarco-Tejada, P.J., Núñez, L.C., Sepulcre-Cantó, G., González, M.R. and Martín, P., 2010. Grape quality assessment in vineyards affected by iron deficiency chlorosis using narrow-band physiological remote sensing indices. *Remote Sensing of Environment*, **114**, 1968-1986.
- Memarsadeghi, N., Mount, D.M., Netanjahu, N.S. and LeMoigne, J., 2007. A Fast Implementation of the ISODATA Clustering Algorithm. *International Journal of Computational Geometry and Applications*, **17**, 71-103.
- Primicerio, J., Di Gennaro, S., Fiorillo, E., Genesisio, L., Lugato, E., Matese, A. and Vaccari, F., 2012. A flexible unmanned aerial vehicle for precision agriculture. *Precision Agriculture*, **13**, 517-523.
- Roberts, D.A., Yamagushi, Y. and Lyon, R.J.P. 1986. Comparison of various techniques for calibration of AIS data. In: *Proceedings, 2nd Airborne Imaging Spectrometer Workshop, Pasadena*. JPL Publication ed.,21-30.
- Rondeaux, G., Steven, M. and Baret, F., 1996. Optimization of soil-adjusted vegetation indices. *Remote Sensing of Environment*, **55**, 95-107.
- Roujean, J.-L. and Breon, F.-M., 1995. Estimating PAR absorbed by vegetation from bidirectional reflectance measurements. *Remote Sensing of Environment*, **51**, 375-384.
- Schneider, V., 2010. Primer on atypical aging. *Wines and Vines*, **4**, 45-51.
- Schultz, H.R. and Löhnertz, O. 2002. Cover crop use in Germany and possible effects on wine quality. . In: *Mondiaviti, Bordeaux*. ITV (FRA) ed., Parisp. 56-64.
- Schultz, H.R. and Stoll, M., 2010. Some critical issues in environmental physiology of grapevines: future

- challenges and current limitations. *Australian Journal of Grape and Wine Research*, **16**, 4-24.
- Smart, R. and Robinson, M., 1991. *Sunlight into wine. A handbook for winegrape canopy management.*, Adelaide, SA, Australia.
- Smit, J.L., Sithole, G. and Strever, A.E., 2010. Vine signal extraction - an application of remote sensing in precision viticulture. *South African Journal of Enology and Viticulture*, **31**, 65-74.
- Smith, G.M. and Milton, E.J., 1999. The use of the empirical line method to calibrate remotely sensed data to reflectance. *International Journal of Remote Sensing*, **20**, 2653-2662.
- Suárez, L., Zarco-Tejada, P.J., Berni, J.A.J., González-Dugo, V. and Fereres, E., 2009. Modelling PRI for water stress detection using radiative transfer models. *Remote Sensing of Environment*, **113**, 730-744.
- Suárez, L., Zarco-Tejada, P.J., González, M.R., Berni, J.A.J., Sagardoy, R., Morales, F. and Fereres, E., 2010. Detecting water stress on fruit quality in orchards with time-series PRI airborne imagery. *Remote Sensing of Environment*, **114**, 286-298.
- Tardaguila, J., Baluja, J., Arpon, L., Balda, P. and Oliveira, M., 2011. Variations of soil properties affect the vegetative growth and yield components of "Tempranillo" grapevines. *Precision Agriculture*, **12**, 762-773.
- Tesic, D., Keller, M. and Hutton, R., 2007. Influence of vineyards floor management practices on grapevine vegetative growth, yield, and fruit composition. *American Journal of Enology and Viticulture*, **58**, 1-11.
- Thenot, F., Méthy, M. and Winkel, T., 2002. The Photochemical Reflectance Index (PRI) as a water-stress index. *International Journal of Remote Sensing*, **23**, 5135-5139.
- Tucker, C.J., 1979. Red and photographic infrared linear combinations for monitoring vegetation. *Remote Sensing of Environment*, **8**, 127-150.
- Zarco-Tejada, P.J., Berjon, A., Lopez-Lozano, R., Miller, J.R., Martin, P., Cachorro, V., Gonzalez, M.R. and de Frutos, A., 2005. Assessing vineyard condition with hyperspectral indices: Leaf and canopy reflectance simulation in a row-structured discontinuous canopy. *Remote Sensing of Environment*, **99**, 271-287.
- Zarco-Tejada, P.J., Berni, J.A.J., Suárez, L., Sepulcre-Cantó, G., Morales, F. and Miller, J.R., 2009. Imaging chlorophyll fluorescence with an airborne narrow-band multispectral camera for vegetation stress detection. *Remote Sensing of Environment*, **113**, 1262-1275.
- Zarco-Tejada, P.J., González-Dugo, V. and Berni, J.A.J., 2012. Fluorescence, temperature and narrow-band indices acquired from a UAV platform for water stress detection using a micro-hyperspectral imager and a thermal camera. *Remote Sensing of Environment*, **117**, 322-337.
- Zarco-Tejada, P.J., González-Dugo, V., Williams, L.E., Suárez, L., Berni, J.A.J., Goldhamer, D. and Fereres, E., 2013a. A PRI-based water stress index combining structural and chlorophyll effects: Assessment using diurnal narrow-band airborne imagery and the CWSI thermal index. *Remote Sensing of Environment*, **138**, 38-50.
- Zarco-Tejada, P.J., Miller, J.R., Morales, A., Berjón, A. and Agüera, J., 2004. Hyperspectral indices and model simulation for chlorophyll estimation in open-canopy tree crops. *Remote Sensing of Environment*, **90**, 463-476.
- Zarco-Tejada, P.J., Morales, A., Testi, L. and Villalobos, F.J., 2013b. Spatio-temporal patterns of chlorophyll fluorescence and physiological and structural indices acquired from hyperspectral imagery as compared with carbon fluxes measured with eddy covariance. *Remote Sensing of Environment*, **133**, 102-115.